

LASER-INDUCED PHOTOACOUSTIC CHARACTERIZATION ON THERMAL DIFFUSIVITY OF CHITOSAN AND SAGO STARCH BIOCOMPOSITE BLEND FILMS

C.K. Sheng^{1✉}, W.M.M. Yunus², W.Md.Z.W. Yunus³, M.Z.Ab. Rahman⁴

¹Faculty of Science and Marine Environment, Universiti Malaysia Terengganu 21030 Kuala Nerus, Terengganu, Malaysia

²Department of Physics, Faculty of Science, Universiti Putra Malaysia, 43400 Serdang, Selangor, Malaysia

³Centre for Tropicalisation, National Defence University of Malaysia, Sungai Besi Camp, 57000, Kuala Lumpur, Malaysia

⁴Department of Chemistry, Faculty of Science, Universiti Putra Malaysia, 43400 Serdang, Selangor, Malaysia

✉ chankoksheng@umt.edu.my

Abstract. The photoacoustic(PA) technique has been testified to be versatile and also reliable for measuring the thermal properties of most materials. For example, it has been utilized to verify the thermal diffusivity of semiconductors, polymers, superconductors, metal, and glass. In this study, the thermal diffusivity of the sago starch and chitosan polymer blend films was characterized using the laser-induced photoacoustic technique. It is based upon the theoretical analysis of the measured photoacoustic signal as a function of light modulation frequency. The value of thermal diffusivity is found to be dependent on the blend composition and further validation was performed through FTIR analysis. The optical transmission spectra show that the blend films process good optical transparency and improved surface quality when compared to the pure sago starch film.

Keywords: chitosan; sago starch; photoacoustic; thermal diffusivity; optical properties

Acknowledgements. *The authors gratefully acknowledge the Faculty of Science, UPM, the Faculty of Science and Marine Environment, UMT, and the Malaysian Government for the help in providing the financial, facilities, advice, and technical assistance on this work.*

Citation: Sheng C.K., Yunus W.M.M., Yunus W.Md.Z.W., Rahman M.Z.Ab. Laser-induced photoacoustic characterization on thermal diffusivity of chitosan and sago starch biocomposite blend films // Materials Physics and Mechanics. 2022, V. 48. N. 1. P. 1-8. DOI: 10.18149/MPM.4812022_1.

1. Introduction

Many polymers can be synthesized with specific properties; however, they often have less desirable characteristics as well. The required property of the polymers can be varied and enhanced by the use of a chemical additive or blending two or more polymers together to meet desired requirements. A polymer composite blend is a macroscopical mixture of two or more different polymers, which is brought about by physically mixing the polymers in the required amounts. The use of composite blends for many technological applications has increased considerably over the last decade as a result of the superior mechanical, electrical,

http://dx.doi.org/10.18149/MPM.4812022_1

© C.K. Sheng, W.M.M. Yunus, W.Md.Z.W. Yunus, M.Z.Ab. Rahman,
2022. Peter the Great St. Petersburg Polytechnic University

This is an open access article under the CC BY-NC 4.0 license (<https://creativecommons.org/licenses/by-nc/4.0/>)

thermal, optical, and other properties of these blends and their favourable cost in comparison to their corresponding individual polymer components [1-7].

Recently, much effort has been made in recent years to develop biodegradable materials, particularly compostable plastics, i.e. plastics that degrade easily under well-defined environmental conditions. These materials may be natural, synthetic, or a combination of both. One of the most studied and relatively new materials for application as a biodegradable plastic is starch, which is a natural renewable polysaccharide obtained from a great variety of crops. Starch is not a true thermoplastic but in the presence of plasticizers, (Water, glycerine, sorbitol, etc.) at high temperatures (90-180°C) and under shear, it readily melts and flows, allowing for its use as an injection, extrusion, or blow moulding material, similar to most conventional synthetic thermoplastic polymers. However, pure thermoplastic starch has some limitations: it is mostly water-soluble and has poor mechanical properties. To improve the desired properties, the use of natural minerals and cellulosic fibres to blend with starch has been considered without interfering in the biodegradability of the composites [5-10].

Over the past few decades, photoacoustic (PA) studies were gradually diffused into a wide range of branches of science, from agricultural and medical sciences to environmental sciences. The PA effect can be detected by enclosing a sample in an airtight cell and exposing it to a modulated beam. As a result of light absorption, the pressure in the air chamber oscillates following the periodic heating of the sample. The resulting pressure fluctuation is detected as PA signal by a sensitive microphone coupled to the cell. The PA technique has been testified to be versatile and also reliable for measuring the thermal properties of most materials. For example, it has been utilized to verify the thermal diffusivity of semiconductors, polymers, superconductors, metal, and glass as well as for direct evaluation of material characteristics variation such as photodegradation and bioprocessing. In addition, it is well known that thermal diffusivity α is the parameter that measures the heat diffusion rate in the material, as given by $\alpha = \kappa / (\rho c)$, where κ is the thermal conductivity, ρ is the mass density and c is the specific heat at constant pressure [11-19]. In this paper, we firstly demonstrated a thorough investigation of the thermophysical properties of the sago starch blend with chitosan biocomposite films using the PA detection technique, which has never been reported before. The samples' optical properties and functional groups were identified by UV-visible spectrophotometer and FTIR spectroscopy, respectively. The aim of this work is to understand the heat diffusion mechanism in the present polymer blends system using the PA technique.

2. Materials and method

Preparation of sample. Chitosan (supplied by UKM) with a deacetylation degree of 88 %, acetic acid (Sigma-Aldrich) and sago starch (Tepung Sago Ind. Ltd., Malaysia) were of analytical grade and used as received without further purification. Acetic acid with a concentration of 1.0 wt.% was used as the solvent for chitosan. Firstly, the required amounts of chitosan (3.00 g, 2.25 g, 1.50 g, and 0.75 g) were dissolved in 100 ml of acid acetic solution and magnetically stirred for 3 hours at 70°C. Simultaneously, the required amounts of sago starch (3.00 g, 2.25 g, 1.50 g, and 0.75 g) were added in 100 ml of distilled water contained in a reaction flask. The homogeneous sago starch solutions were obtained after constant stirring at 80°C for half an hour. The blend solutions of chitosan and sago starch were mixed in the reaction flask and then immersed in a circulating water bath at a temperature of 80°C for 5 hours. Finally, the blend films were obtained by drying the solution in a petri dish at room temperature for 10 days. The composition of chitosan and sago starch blends were prepared in various compositions as listed in Table 1. The average thicknesses of these biofilms were in the range of 0.030-0.045 mm.

Table 1. Compositions of sago starch and chitosan blend films

Samples	Amount of chitosan	Amount of sago starch
SSC 100-0	0 g (0%)	3.00 g (100%)
SSC 75-25	0.75 g (25%)	2.25 g (75%)
SSC 50-50	1.50 g (50%)	1.50 g (50%)
SSC 25-75	2.25 g (75%)	0.75 g (25%)
SSC 0-100	3.00 g (100%)	0 g (0%)

Photoacoustic measurement. The schematic experimental set-up for the photoacoustic measurement is depicted in Fig. 1. The 75 mW helium-neon laser beam, which after being mechanically chopped by an optical chopper (SR540) was focused onto the sample kept inside a non-resonant PA cell. The cell was fitted with an electret microphone (Cirkit product, UK) and covered with a silica glass window. As a result of the periodic heating of the sample by the absorption of the modulated light, the heat generated in the sample is transferred to the gas in contact. Hence, the pressure fluctuations in the air chamber oscillate with the chopping frequency that can be detected by the microphone as PA signal. Eventually, the generated PA signal is amplified by a preamplifier (SR560) and further analyzed by a lock-in amplifier (SR530). The PA signal amplitude is recorded as a function of the modulation frequency.

The theory of the photoacoustic effect in a solid sample was first described by Rosenwaig and Gersho (R-G) [12,13], and according to the R-G model, the heat generated in the sample will diffuse from the sample to the gas in immediate contact with the sample. An important parameter involved is the thermal diffusion length of the sample μ_s , which can be defined in terms of the thermal diffusivity by equation (1) as:

$$\mu_s = \sqrt{\alpha / (\pi f)}. \quad (1)$$

From the equation, the μ_s decreases with the increasing modulation frequency. The modulation frequency is termed as characteristic frequency, f_c ($f = f_c$) when the thermal diffusion length, μ_s becomes equal to sample thickness, l_s ($\mu_s = l_s$). According to the value of frequency, we may distinguish two regimes: below f_c and above f_c . When ($f < f_c$) or ($\mu_s > l_s$) for a thermally thin sample, the amplitude of the photoacoustic (PA) signal decreases as f^{-1} one decreases the modulation frequency. In contrast, at high modulation frequencies ($f > f_c$) or ($\mu_s < l_s$) for the thermally thick sample, the amplitude of PA signal varies as $f^{-1.5}$. Hence, by knowing f_c and l_s , the thermal diffusivity can then be attained by applying equation (2) as given below:

$$\alpha_s = \pi f_c l_s^2. \quad (2)$$

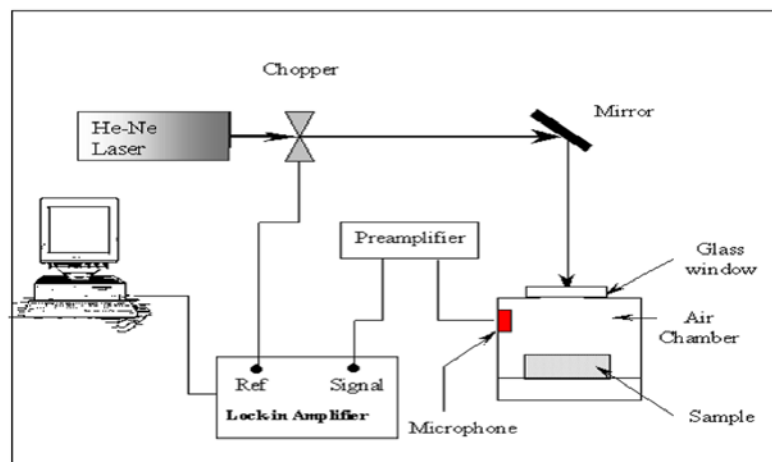


Fig. 1. The schematic experimental set-up for the photoacoustic measurement

FTIR analysis. The structural bonding of all the blend films was determined by FTIR analysis using Perkin Elmer 720 FTIR spectrometer. The IR transmission spectra of the film were recorded between 400 cm^{-1} and 4000 cm^{-1} at room temperature with a spectral resolution of 1 cm^{-1} .

Optical properties. The optical transmission spectra of the sample were recorded by employing a fiber optics spectrophotometer (OCEAN Optics, Inc.) with a UV-visible light source in the wavelength region of 350-750 nm.

Thickness measurement. The sample thickness was measured by a digital micrometer model DTG03L, which is a digital thickness gauge with extended reach intended for measurements at up to 120 mm (4.7") from the edge of film or sheet material. The accuracy of the device to measure the sample thickness gives resolution down to 1 micron (0.001mm). The sample thickness was determined in several points of the sample and take an average of these measurements as the sample thickness which was repeated 5 times.

3. Results and Discussion

The photoacoustic signals were measured in the (5-150) Hz modulation frequency range. The typical plots of the PA signal amplitude as a function of modulation frequency for the pure sago starch and the blend containing 75% sago starch and 25% chitosan (SSC 75-25) are depicted in Fig. 2 (a) and (b), respectively. From the figure, the PA signal is quite prominent at a lower frequency and exhibits a rapid exponential drop as the frequency modulates at a higher rate. The PA signal detected at lower frequencies is principally attributed to the thermo-optical effect that occurs deep below the sample surface, however, as the modulation frequency increases, the detected PA signal is predominantly contributed by the surface vibration due to the propagation of light within the blend film surface before another heat pulse begins. The frequency response of an electret condenser microphone is usually in the range of 20 Hz–20 kHz. Thus, the PA signal analysis selected in this study for thermal diffusivity is mainly lying in the range of the frequency response.

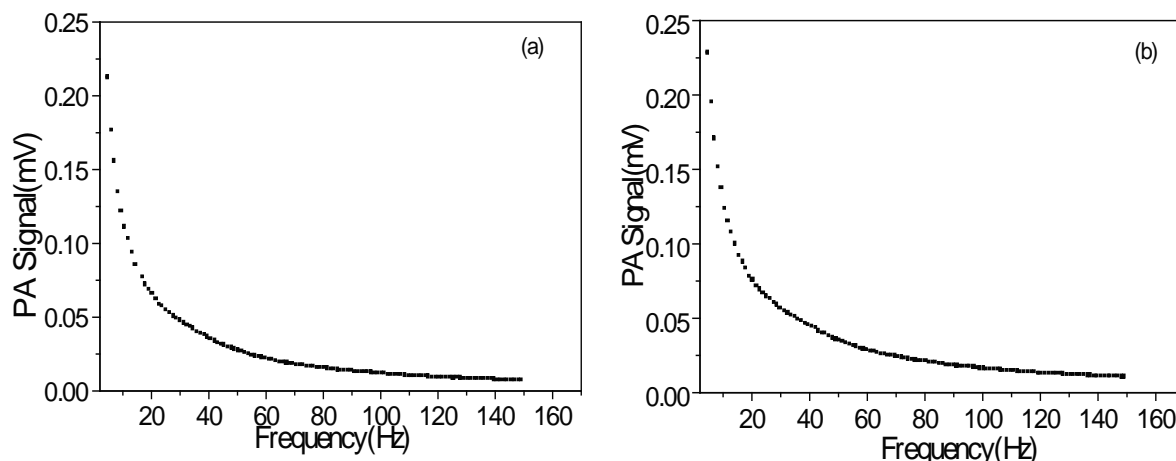


Fig. 2. PA signal versus frequency for the samples of (a) SSC 100-0 and (b) SSC 75-25

The examples of the plot of $\ln(\text{PA signal})$ versus $\ln(\text{frequency})$ for SSC 100-0 and SSC 75-25 are presented in Fig. 3, whereby the f_c values are respectively determined as 36.23 and 37.34. Accordingly, the thermal diffusivity values of these samples were calculated by substituting the f_c and l_s values into Equation (2). Thermal diffusivity values for the other blends of chitosan and sago starch were determined using a similar method and were tabulated in Table 2. The results reveal that the thermal diffusivity values of the blends of sago starch and chitosan are lied in the range of 1.44×10^{-3} - $2.01 \times 10^{-3}\text{ cm}^2/\text{s}$. These values are

in agreement with the thermal diffusivity range obtained for the polymeric film as reported previously by Hashimoto et al. [20]. Apparently, the thermal diffusivity of pure chitosan ($2.26 \times 10^{-3} \text{ cm}^2/\text{s}$) is determined higher than the pure sago starch ($1.17 \times 10^{-3} \text{ cm}^2/\text{s}$). For the sago starch and chitosan blends, the thermal diffusivity values obtained were higher than pure sago starch but lower than pure chitosan. Furthermore, it is also discovered that the thermal diffusivity value increases proportionally with the amount of chitosan added to the blend film. This characteristic can be associated with the formation of intermolecular hydrogen bonds between NH^{3+} of the chitosan backbone and OH^- of the starch that facilitates the heat transfer through the blend film [21].

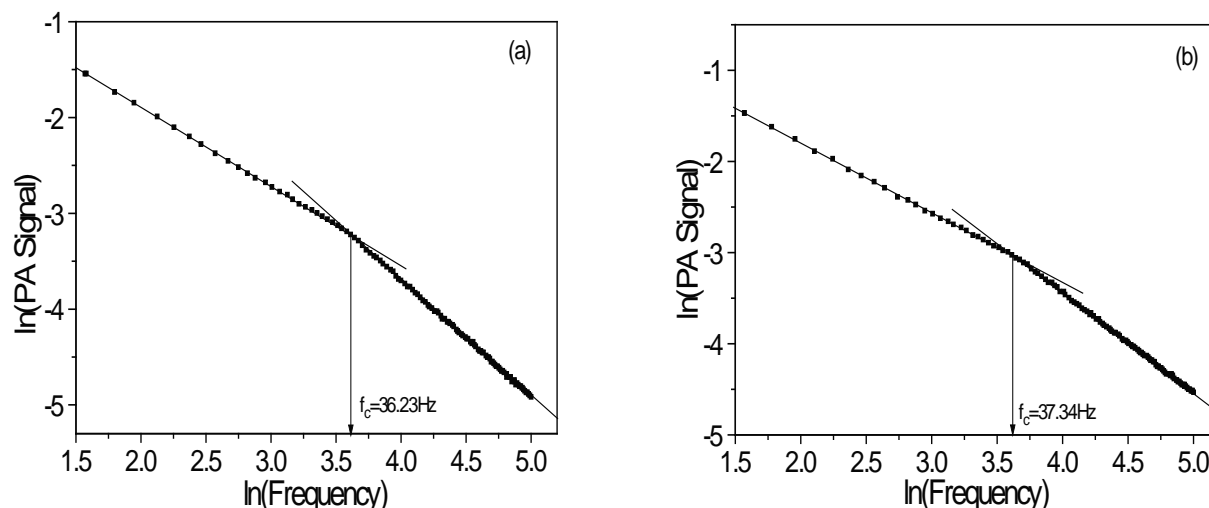


Fig. 3. $\ln(\text{PA signal})$ versus $\ln(\text{frequency})$ for (a) SSC 100-0 and (b) SSC 75-25

Table 2. Thermal diffusivity values of the sago starch-chitosan blends

Samples	Thermal diffusivity ($\times 10^{-3} \text{ cm}^2/\text{s}$)
SSC 100-0	1.17 ± 0.01
SSC 75-25	1.44 ± 0.01
SSC 50-50	1.72 ± 0.01
SSC 25-75	2.01 ± 0.02
SSC 0-100	2.26 ± 0.02

The formulated film's surface was clearly seen smooth and homogeneous as observed with the naked eye. The FTIR analysis was carried out to determine the molecular bonding structure of the sago starch and chitosan blends. The measured FTIR spectra of the chitosan and sago starch blends are displayed in Fig. 4. From the observation, the spectra of all blends are quite similar. This result implies that there is no formation of a new bond within the blends. Basically, the FTIR spectra for the blend samples are more similar to sago starch if the content of the sago starch is higher than chitosan. On the other hand, the observed trend is more similar to the spectra of the pure chitosan if the percentage of chitosan is higher than sago starch. From the FTIR spectra, all the intensity of peaks at around 3415 cm^{-1} (N-H stretching), 2988 cm^{-1} (C-H stretching), 1635 cm^{-1} (O-H bending), 1526 cm^{-1} (CH_2 bending) 1397 cm^{-1} (C-H bending), and 701 cm^{-1} (N-H bending) becomes stronger and broader with the increase of chitosan in the blend films [7, 8, 21-26]. This feature might contribute to the increase of thermal diffusivity values when higher chitosan content is added into the blends since the chitosan possesses better conductivity as compared to starch. Furthermore, from the FTIR analysis results, it is worthy to deduce that the blending process for the chitosan and

sago starch is through physical interaction only. This is because there is no new absorption peak exists from the spectra due to the chemical bonding between chitosan and sago starch.

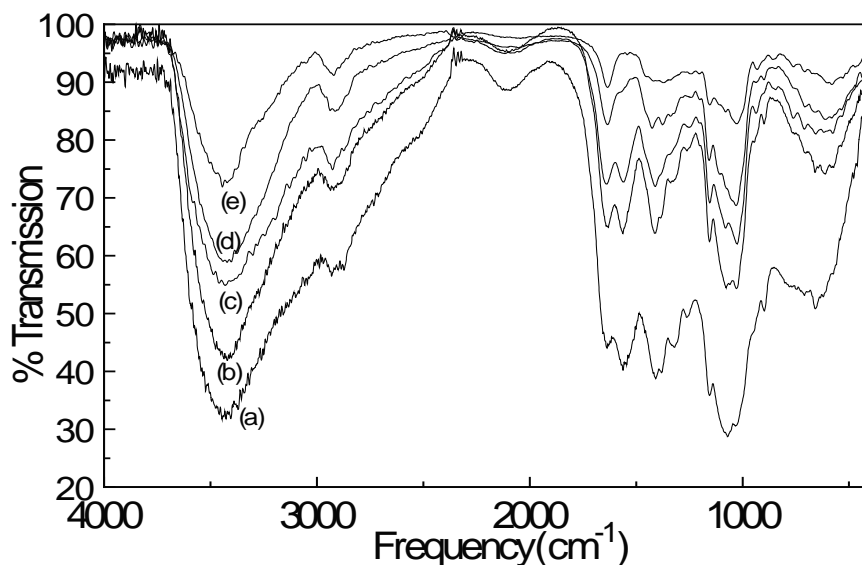


Fig. 4. FTIR spectra of chitosan and sago starch blends: (a) SSC 0-100; (b) SSC 25-75; (c) SSC 50-50; (d) SSC 75-25; (e) SSC 100-0

Subsequently, the optical transmission spectra of the present blend films are characterized using a fiber optics spectrophotometer as presented in Fig. 5. From the figure, it could be observed that the blend films show a good optical transmission of within (72-87) % in the visible and near IR range from 500 nm to 850 nm. Nevertheless, the transmission of pure starch is determined to be 41% only, which is much lower as compared to the blend films and pure chitosan (87%). Also, there are absorption edges present in the UV and visible region of 350–500 nm and these edges become gradually steeper as the content of chitosan increases in the blend. Moreover, a small peak of transmission occurred at a wavelength of 579 nm for all the samples, indicating effective optical transmittance at this wavelength. As a consequence, the result implies that the blend films offer an improved surface quality and good optical transparency when compared to pure starch.

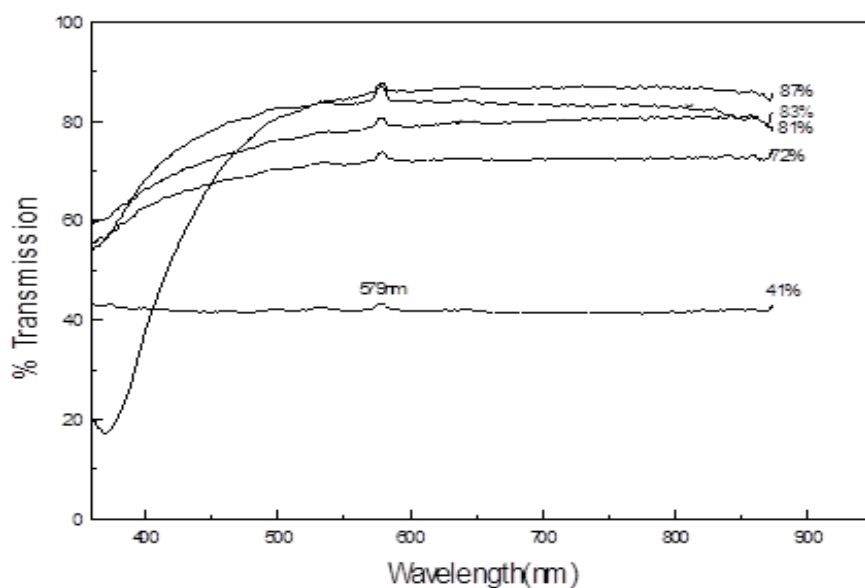


Fig. 5. Optical transmission spectra of chitosan and sago starch blends

4. Conclusions

In summary, we have successfully demonstrated the availability of the photoacoustic (PA) technique for measuring the thermal diffusivity of the sago starch and chitosan blend films. From the results obtained, it is found that the thermal diffusivity of pure chitosan is higher than the pure sago starch and the thermal diffusivity value increases with the increasing of chitosan contents in the blends. Also, the transmission spectra show that a good surface quality and high optical transparency are attained for the present blend films. From the FTIR spectra, all the intensity of peaks become stronger and broader due to an improved physical interaction between sago starch and chitosan.

References

- [1] Dorel F, Barbalata A. *Technology, properties and applications of polymers*. London, UK: Chapman and Hall Publishers; 1995.
- [2] Sheng CK, Amin KAM, Kee KB, Hassan MF, Ali EGE. Effect of wood flour content on the optical color, surface chemistry, mechanical and morphological properties of wood flour/recycled high density polyethylene (rHDPE) composite. *AIP Conference Proceeding*. 2018;1958(1): 1-10.
- [3] Lu DR, Xiao CM, Xu SJ. Starch-based completely biodegradable polymer materials. *Express Polymer Letter*. 2009;3(6): 366-375.
- [4] Sheng CK, Amin KAM, Hong LL, Hassan MF, Ismail M. Investigation of morphological, structural and electrical properties of Cds/ PMMA nanocomposite film prepared by solution casting method. *International Journal of Electrochemical Science*. 2017;12: 10023-10031.
- [5] Gatenholm P, Mathiasson A. Biodegradable natural composites. II. Synergistic effects of processing cellulose with PHB. *Journal of Applied Polymer Science*. 1995;51(7): 1231-1237.
- [6] Yoon SD, Park MH, Byun HS. Mechanical and water barrier properties of starch/PVA composite films by adding nano-sized poly(methyl methacrylate-co-acrylamide) particles. *Carbohydrate Polymer*. 2012;87(1): 676-686.
- [7] Azahari NA, Othman N, Ismail H. Biodegradation studies of polyvinyl alcohol/corn starch blend films in solid and solution media. *Journal of Physical Science*. 2011;22(2): 15-31.
- [8] Sheng CK, Senin H, Naimah BI. Structural and mechanical properties of polyvinyl alcohol (PVA) thin film. *AIP Conference Proceeding*. 2009;1136: 366-369.
- [9] Yao K, Cai J, Liu M, Yu Y, Xiong H, Tang S, Ding S. Structure and properties of starch/PVA/nano-SiO₂ hybrid films. *Carbohydrate Polymer*. 2011;86(4): 1784-1789.
- [10] Tang X, Alavi S. Recent advances in starch, polyvinyl alcohol based polymer blends, nano composites and their biodegradability. *Carbohydrate Polymer*. 2011;85(1): 7-16.
- [11] Lima CAS, Lima MBS, Miranda LCM, Baeza J, Freer J, Reyes N, Ruiz J, Silva MD. Photoacoustic characterization of bleached wood pulp and finished papers. *Measurement Science and Technology*. 2000;11(5): 504-508.
- [12] Rosencwaig A, Gershon A. Theory of the photoacoustic effect with solid. *Journal of Applied Physics*. 1976;47(1): 64-69.
- [13] Perondi LF, Miranda LCM. Minimal-volume photoacoustic cell measurement of thermal diffusivity: Effect of the thermoelastic sample bending. *Journal of Applied Physics*. 1987;62(7): 2955.
- [14] Sheng CK, Yunus WMM, Yunus WMZW, Talib ZA, Kassim A. characterization of thermal, optical and carrier transport properties of porous silicon using photoacoustic technique. *Physica B: Condensed Matter*. 2008;403(17): 2634-2638.
- [15] Yunus WMM, Sheng CK, Yunus WMZW. Study on photobleaching of methylene blue doped in PMMA, PVA and gelatin using photoacoustic technique. *Journal of Nonlinear Optical Physics & Materials*. 2003;12(1): 91-100.

- [16] Sheng CK, Yunus WMM, Yunus WMZW. Measurement of thermal diffusivity, optical transmission and optical absorption peaks of laser dyes R6G doped in poly(methylmethacrylate) using photoacoustic technique and fibre optics spectrophotometer. *Pertanika Journal of Science & Technology*. 2003;11(1): 83-91.
- [17] Sheng CK, Yunus WMM, Talib ZA, Tarmizi EZM. Photoacoustic measurement of thermal diffusivity of coconut shell. *Journal of Solid State Science and Technology Letters*. 2006;13(1): 243-248.
- [18] Da Silva MD, Bandeira IN, Miranda LCM. Open-cell photoacoustic radiation detector. *Journal of Physics E: Scientific Instruments*. 1987;20(12): 1476-1478.
- [19] Da Costa ACR, Siqueira AF. Thermal diffusivity of conducting polypyrrole. *Journal of Applied Physics*. 1996;80(10): 5579-5582.
- [20] Hashimoto T, Matsui Y, Hagihara A, Miyamoto A. Thermal diffusivity measurement of polymer films by the temperature wave method using joule-heating. *Thermochimica Acta*. 1990;163: 317-324.
- [21] Xu YX, Kim KM, Hanna MA, Nag D. Chitosan–starch composite film: preparation and characterization. *Industrial Crops and Products*. 2005;21(2): 185-192.
- [22] Sheng CK, Alrababah YM. The Role of pH on Infrared Spectral, Structural and Morphological Properties of Room-temperature Precipitated CdS Nanoparticles. *Journal of Nano- and Electronic Physics*. 2020;12(1): 01017.
- [23] Alrababah YM, Sheng CK, Hassan MF. Influence of ammonium nitrate concentration on structural evolution and optical properties tuning of CdS nanoparticles synthesized by precipitation method. *Nano-Structures & Nano-Objects*. 2019;19: 10034.
- [24] Ali EAGE, Kim TL, Abdullah MAA, Sheng CK. Effects of graphite milling time and composition to tensile properties of poly-methyl methacrylate (PMMA)/graphite composite. *Journal of Sustainability Science and Management*. 2019;14(6): 4-11.
- [25] Dris MRM, Sheng CK, Isa MIN, Razali MH. A study of cadmium sulphide nanoparticles with starch as a capping agent. *International Journal of Technology*. 2012;1: 1-7.
- [26] Sheng CK, Senin HB, Hamdan S. Mechanical properties of Malaysian Cengal wood as dried sample and under fiber saturated point. *AIP Conference Proceeding*. 2008;1017(1): 286-289.

THE AUTHORS

Sheng C.K.

e-mail: chankoksheng@umt.edu.my

ORCID: 0000-0003-2020-4759

Yunus W.M.M.

e-mail: chankoksheng@umt.edu.my

ORCID: -

Yunus W.Md.Z.W.

e-mail: wanmdzin@upnm.edu.my

ORCID: -

Rahman M.Z.Ab.

e-mail: chankoksheng@umt.edu.my

ORCID: -